REPORT DOCUMENTATION PAGE

Form Approved OMB No. 0704-0188

1. AGENCY USE ONLY (Leave blank)	2. REPORT DATE	3. REPORT TYPE AND DATES COVERED
	June 1997	Final Report

4. TITLE AND SUBTITLE

Mirror Coronagraphic Device - Development and Manufacture of a Reflecting Coronagraphic Device for Application in a Low-Scattered Light Telescope

5. FUNDING NUMBERS

F6170894W0743

6. AUTHOR(S)

Dr Iraida S. Kim

7. PERFORMING ORGANIZATION NAME(S) AND ADDRESS(ES)

Sternberg Astronomical Institute
Universitetetsky Prospect, 13
Moscow 119899
Russia

8. PERFORMING ORGANIZATION REPORT NUMBER

N/A

9. SPONSORING/MONITORING AGENCY NAME(S) AND ADDRESS(ES)

EOARD
PSC 802 BOX 14
FPO 09499-0200

10. SPONSORING/MONITORING AGENCY REPORT NUMBER

SPC 94-4078

11. SUPPLEMENTARY NOTES

12a. DISTRIBUTION/AVAILABILITY STATEMENT

Approved for public release; distribution is unlimited.

12b. DISTRIBUTION CODE

A

13. ABSTRACT (Maximum 200 words)

This report results from a contract tasking Sternberg Astronomical Institute as follows: Development and manufacture of a reflecting coronagraphic device for application in a low-scattered light telescope suitable for detection of very faint astronomical objects in the presence of bright ones.

14. SUBJECT TERMS	15. NUMBER OF PAGES
	15
	16. PRICE CODE N/A

17. SECURITY CLASSIFICATION OF REPORT	18. SECURITY CLASSIFICATION OF THIS PAGE	19, SECURITY CLASSIFICATION OF ABSTRACT	20. LIMITATION OF ABSTRACT
UNCLASSIFIED	UNCLASSIFIED	UNCLASSIFIED	UL

NSN 7540-01-280-5500

Standard Form 298 (Rev. 2-89)
Prescribed by ANSI Std. 239-18
298-102

THE FINAL REPORT

Contract Number F6170894W0743 (SPC-94-4078)
"Mirror coronagraphic device" - development and manufacture of a reflecting coronagraphic device for application in a low-scattered light telescope suitable for detection of a very faint astronomical objects in the presense of bright ones

To the end of 1996 two additional pin-hole inverse occulting disks (Figure 1) with diameter of 0.5 and 1 mm as well a dustproof duralumin cover have been manufactured. Finally, the coronagraphic device may be used both for day time and for night time observations.

Researches of scattered light of the device were made recently. As a rule the intensity of the object under study in the final focal plane as a function of distance from the the center of the Airy disk may be described by the Point Spread Function (PSF) of the telescope.
Generally PSF of the device is mainly caused by:

a. Optics aberrations;
b. Diffraction at the edge of the entrance purple;
c. Scattering at the micro-roughness of the primary optics.

1. Optics aberrations

As mentioned before (Preliminary report) two halves of the 20-cm Si-mono-crystalline super-smooth on-axis mirror are used as a primary off-axis mirror and a field off-axis mirror. Such an optical configuration results in minimizing aberrations caused by coma and astigmatism.

Optics aberrations of the device have been calculated and are shown in Figures 2-5.

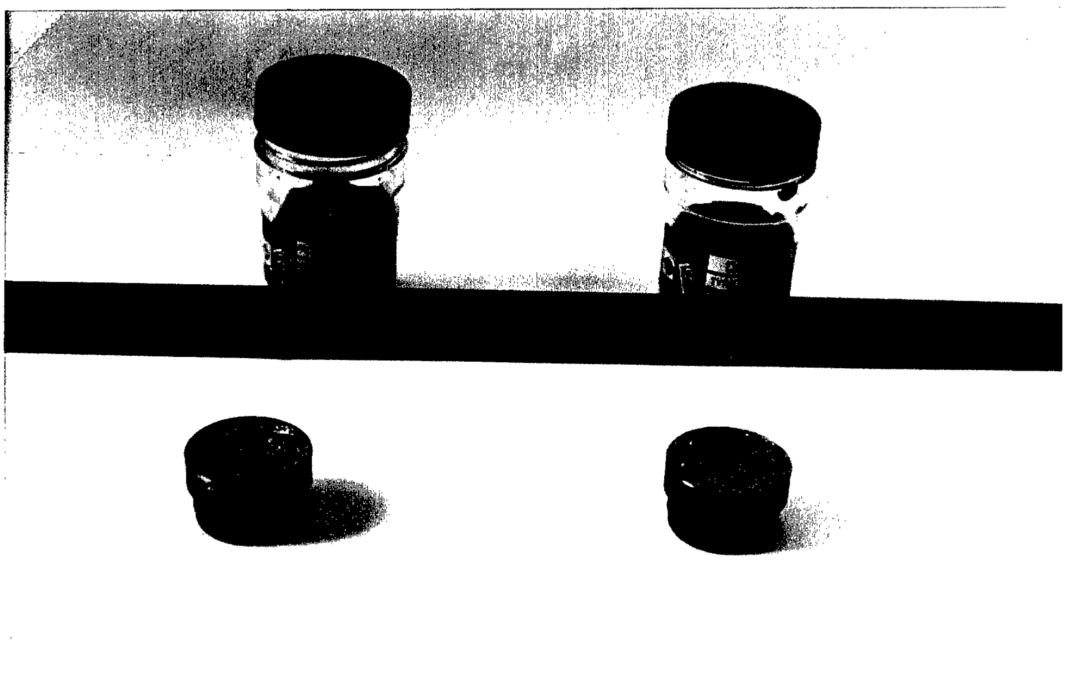

Figure 1. Pin-hole inverse occulting disks with diameter of 0.5 and 1 mm allowing employment of the device for night-time astronomy. The disks are coated by protective films.

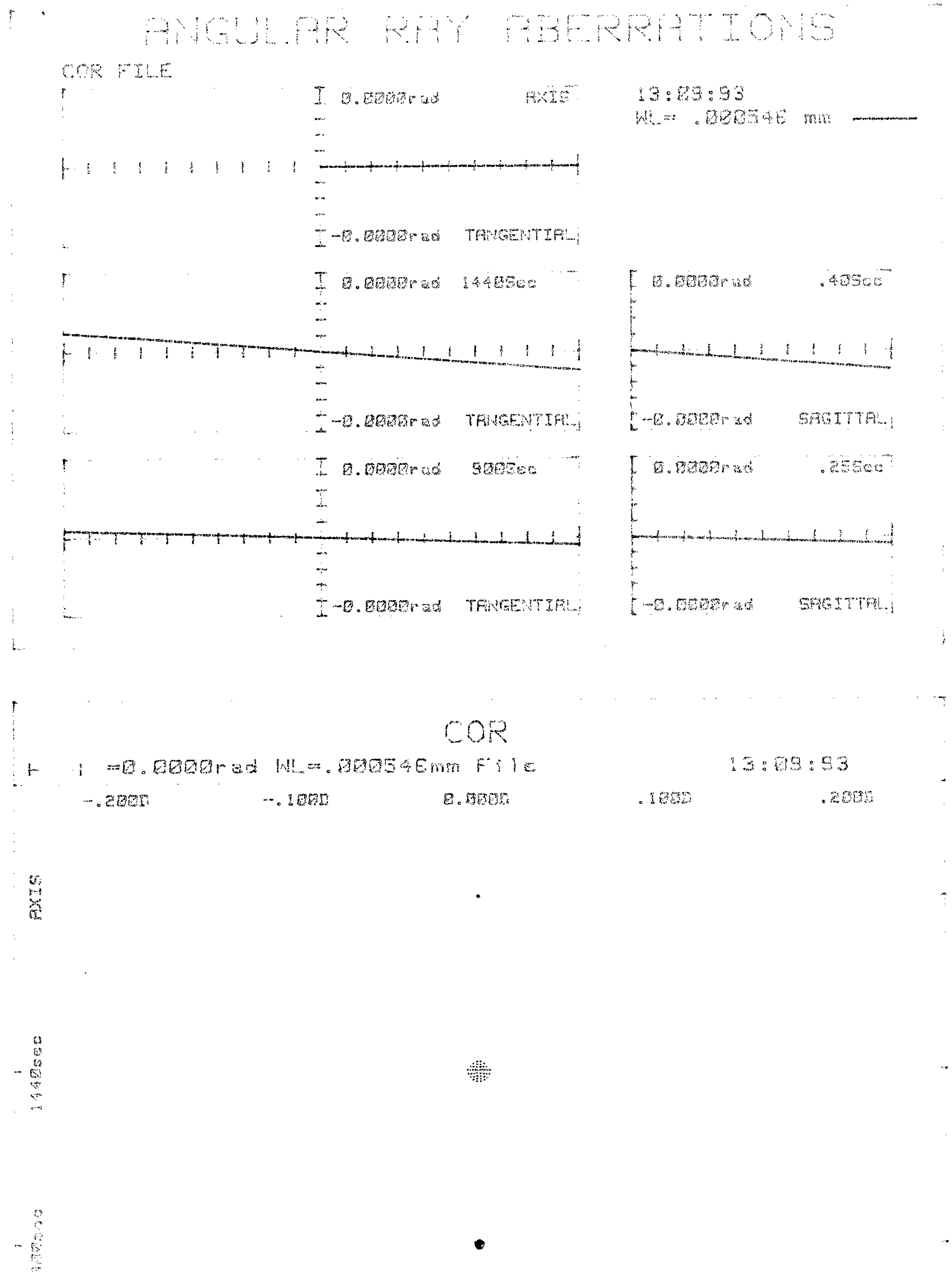

Figure 2. Angular ray aberrations of the coronagraphic device.

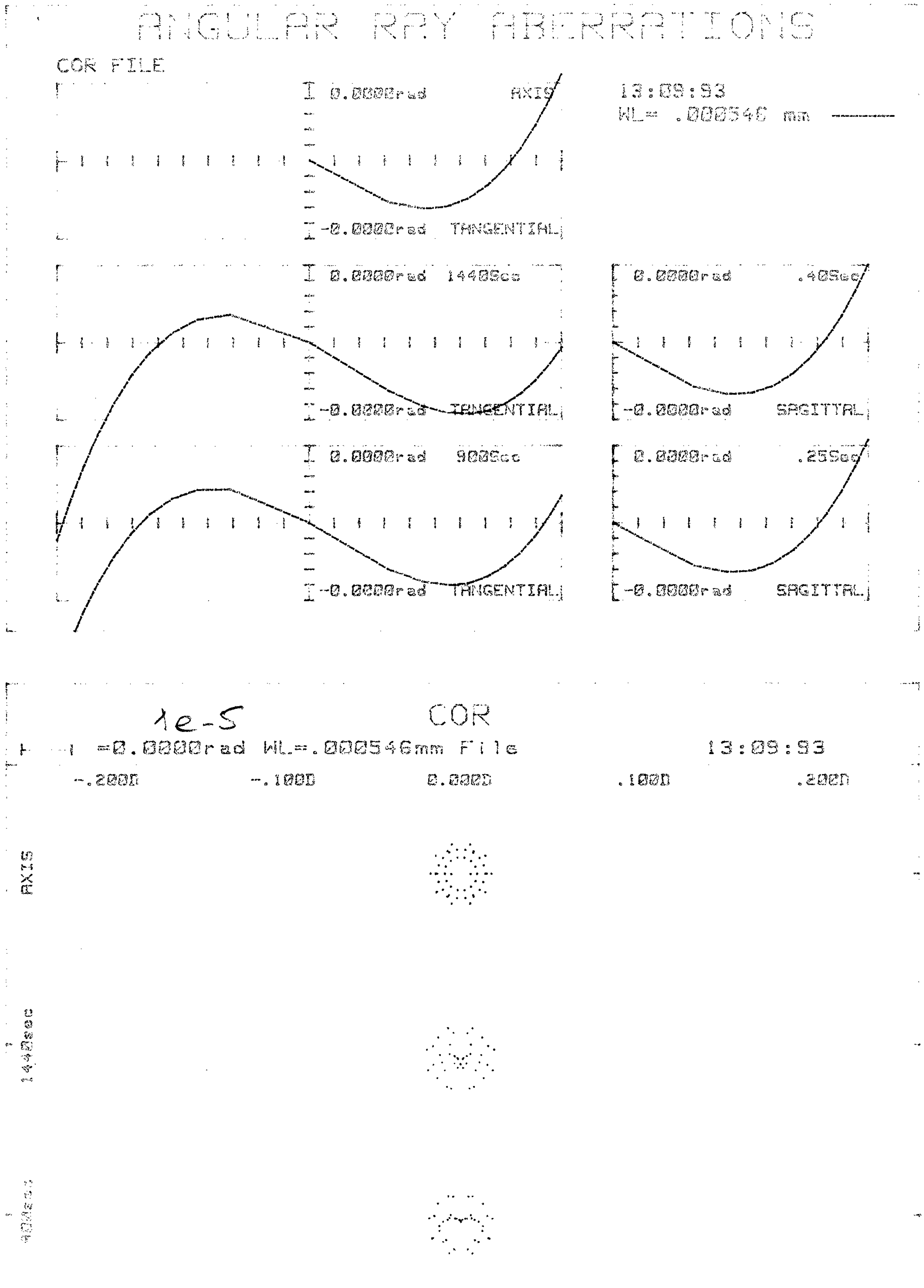

Figure 3. Angular ray aberrations of the coronagraphic device.

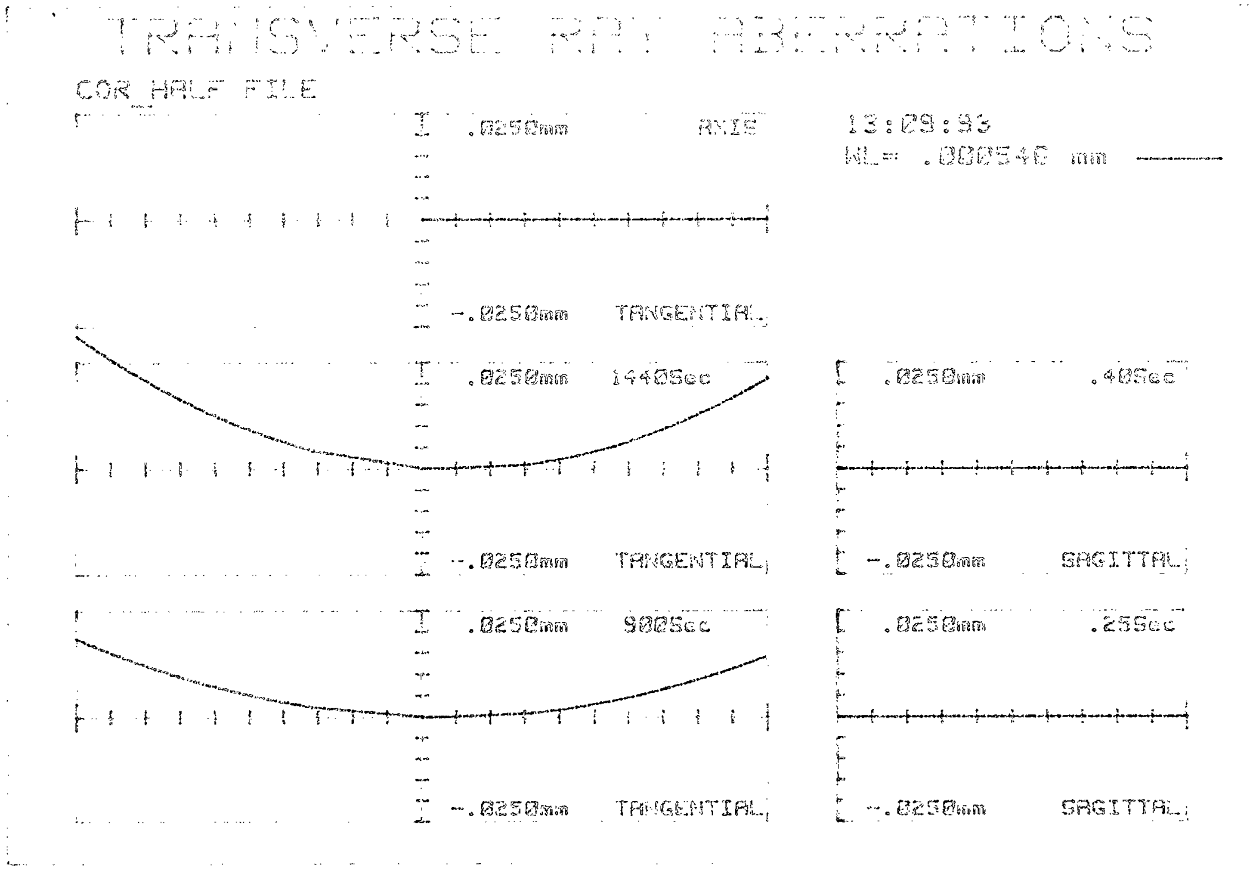

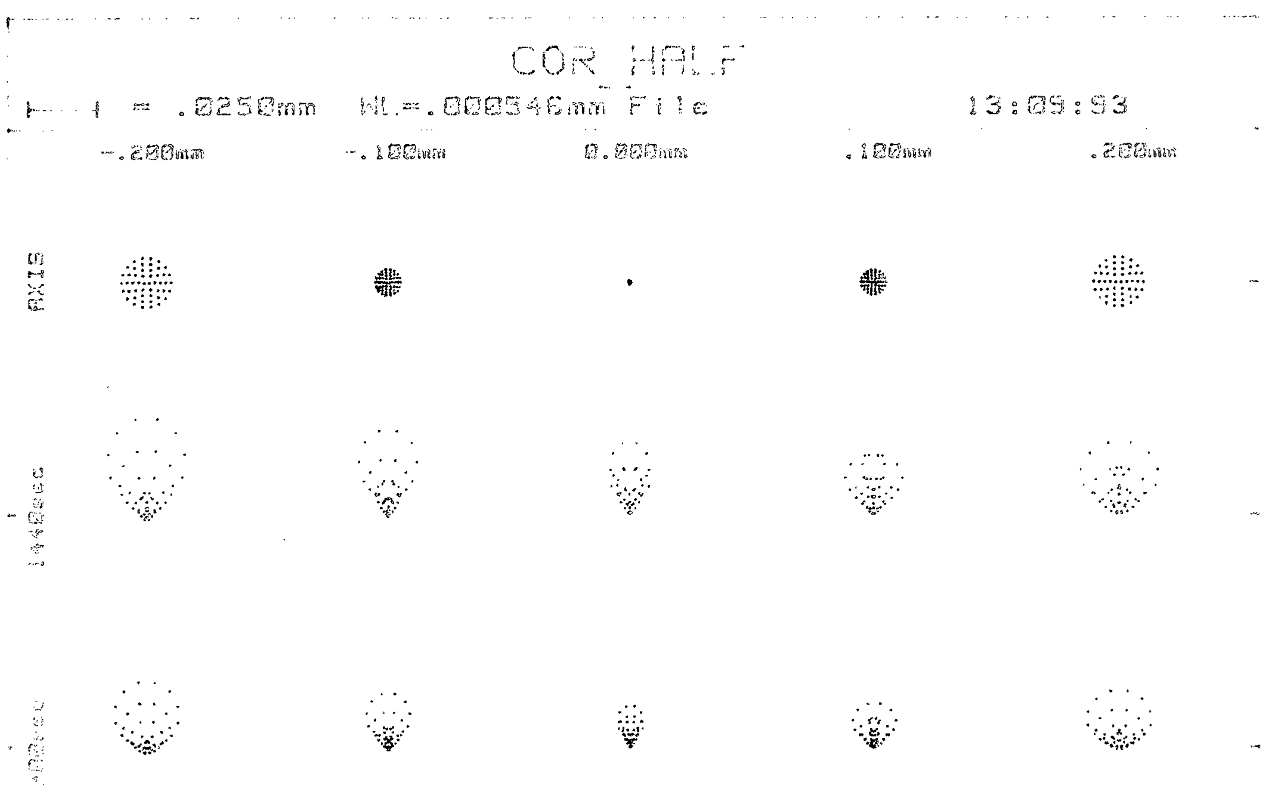

Figure 4. Transverse ray aberrations of the coronagraphic device.

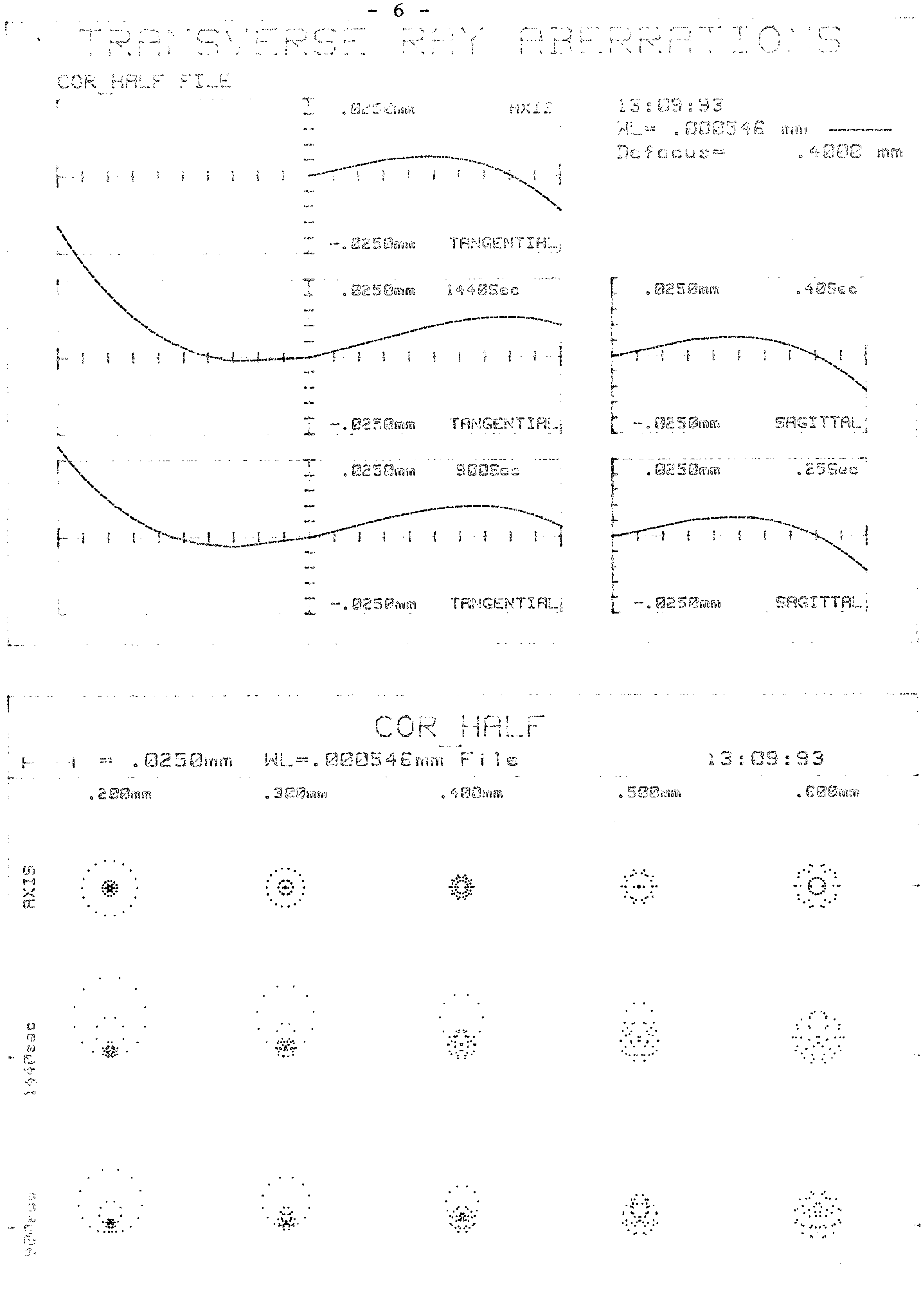

Figure 5. Transverse ray aberrations of the coronagraphic device.

2. Diffraction at the edge of the entrance pupil

Generally PSF being a square of modulus of corresponding equation of convolution is calculated by re-iterated employment of algorithm of Fast Fourier Transform requiring for the 2D case huge volume of calculations. PSF of an ideal (in sense of optics aberrations and roughness) coronagraphic telelescope having an occulting disc and a Lyot stop will depend on several parameters: shape of the entrance pupil, ratio of "radius of entrance pupil-to-radius of exit pupil", etc.

For an ideal optics PSF can be simplified. Let R = D/2 be a radius of a round entrance aperture, r - radius of an occulting disk, A - ratio of "radius of exit pupil-to-radius of entrance pupil". Then the convolution equation written in polar reference and normalized to the brightness at the center of Airy pattern takes the form:

$$E(u,\beta) \equiv E(u) = \int_0^{2\pi}\int_r^{\infty} \frac{2J_1(Av)}{Av}\,\frac{J_1(w)}{2\pi w}\, v\,dv\,d\alpha,$$

where $u = \frac{2\pi}{\lambda}\frac{R}{A}\psi$ - radial coordinate depending on the angle of scattering and on the wavelength λ, $J_1(x)$ - Bessel function, and $w = \sqrt{v^2+u^2-2uv\cos\alpha}$.
Using the theorem of adding the Bessel functions the convolution is transformed to a fast convergent series

$$E(u) = \sum_{l=0}^{\infty} g_l \frac{J_{2l+1}(u)}{u},$$

of which factors are convinient for computering by integrals for the whole complex of of R, r, and A values:

$$g_l = 4(2l+1)\int_r^{\infty} \frac{J_1(Av)}{Av} J_{2l+1}(v)\,dv.$$

3. Testing the primary mirror

Micro-relief of the primary optics of the device was examinated to study the behaviour of PSF versus on micro-relief.
It's known that spatial structute of micro-relief of an optical surface is mainly caused by technology of polishing. That's why spatial structure of the 20-cm Si-mono-crystalline super-smooth was studied using several examples (with diameters of 10 mm) polished by the same technology. The examples were measured by a "Wyko type non-contact surface profiler".

Two scans made at perpendicular directions foe one of the examples are shown in Figure 6. RMS of micro-roughness is found to be less than 5 A. The spatial structure of micro-relief evidently reveals the quasi-regular spatial structure which may be caracterized by a size of about 20 (18) and 100 micron. That means that for the first approximation micro-relief of the reflecting primary optics of the device may be represented by superposition of sinusoidal phase gratings with a deep of RMS and a grating constant of 20 and 100 micron.

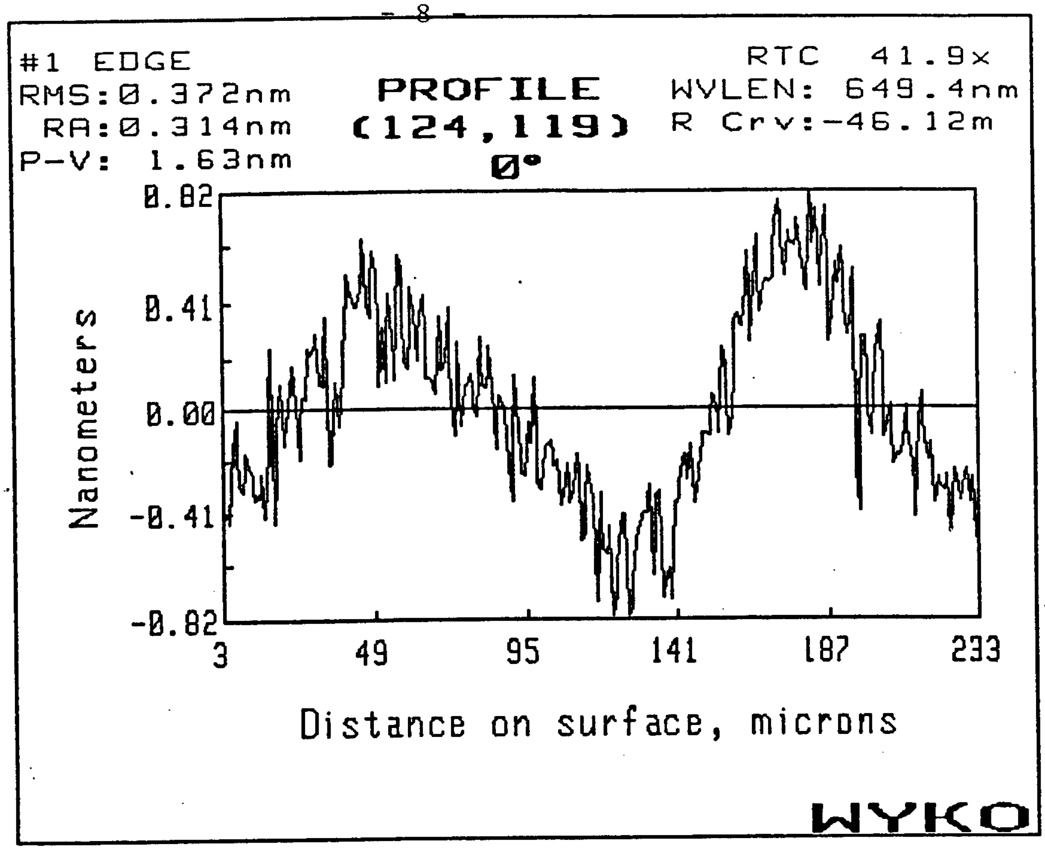

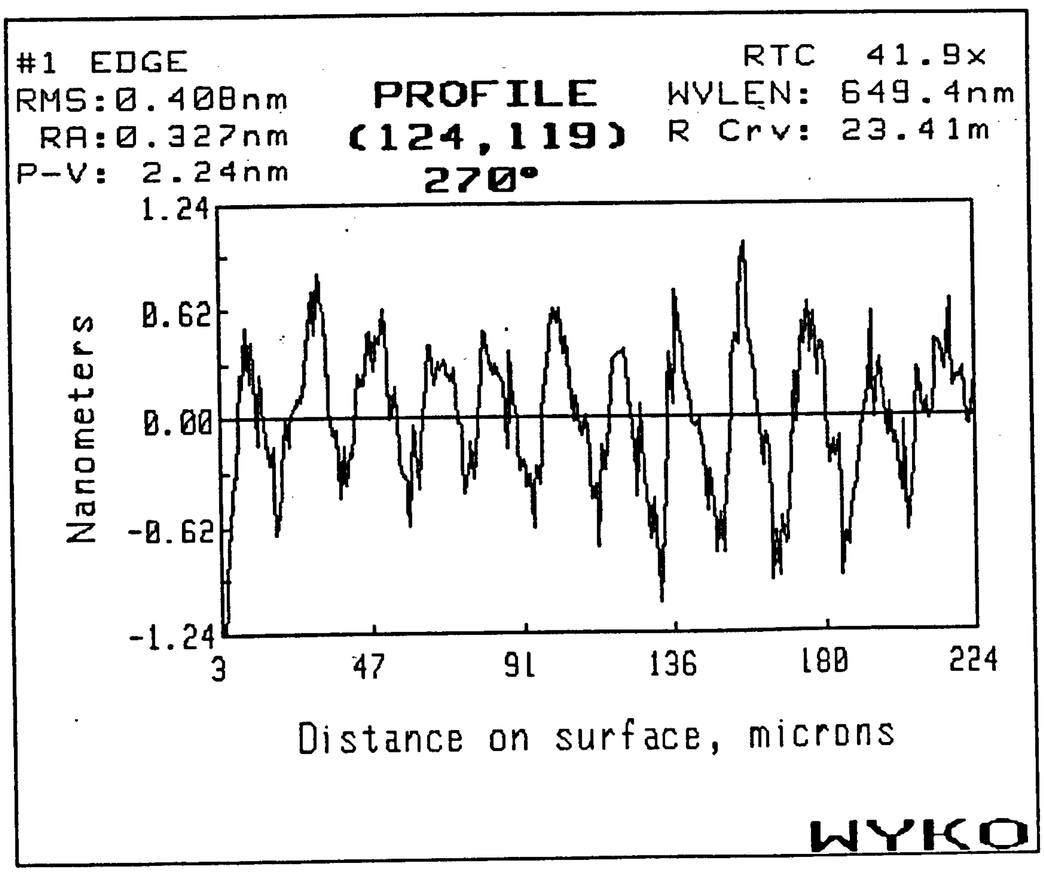

Figure 6. Measurements of micro-relief.

4. Scattering at micro-roughness of the primary optics

For reflecting coronagraphs the most significant input of the scattered light would be caused by micro-roughness of the primary optics. Below corresponding calculations are presented for solar applications in the range 1.16 -2.0 Ro (solar radius). The limb darkening was neglected.

The theory of the scattering of electromagnetic waves from rough surfaces was presented in detail elsewhere (Beckmann et al., 1963; Wazerell, 1983; Toporets, 1988; Faure-Geors et al., 1988).

For the first approximation an approach of phase grating may be used (Romanov et al., 1991). A phase grating represents grating with periodically varying delay of the wave front. Micro-relief of a reflecting primary optics is represented by superposition of sinusoidal phase gratings with a deep of "a" and a grating constant "d".

The first step of the program consists of computation of PSF for a given function of the wave front. Let be rotating symmetry of a phase grating centering relative to a round entrance aperture. The function of errors of a wave front is given by expression:

$$W(\rho) = a\cos(2\pi b\rho + \varphi) ,$$

where b = d/r - spatial frequancy of a phase grating measured in periods in units of radius of entrance pupil, ρ - normalized radius of an entrance pupil, φ - the phase angle while ρ = 0. PSF of the above-mentioned system contents a circular structure. The radius of the circle, its width, maximum of relative intensity within the band of the nth order is determined by formulas given by Wazerell (1998).

The second step of the program represents computations of PSF in the range 1.16-2.0 Ro. The solar disk was represented by elementary areas. PSF was calculated for the center of each area. The input of the area in a resulting PSF was determined by its PSF multiplied by corresponding weight factor.

Validaty of the program was checked by comparison of PSF corresponding to an ideal optics (W (ρ) = 0) and PSF according to Nagaoka (1920) A complete coincidence of numerical modeling and analytical solution was found.

Table 1 and Figure 7 represent computations made for diameter of the entrance aperture of 20 cm, effective wavelength of 530.3 nm, phase grating constant of 5, 10, 20, 50, 100 micron, and micro-roughness of 10 A.
It's seen that PSF does not practically depend on spatial parameters.

Table 2 and Figure 8 represent similar computations made for diameter of the entrance aperture of 20 cm, effective wavelength of 530.3 nm, phase grating constant of 5, 10, 20, 50, and 100 micron, and micro-roughness of 20 A.
PSF varies from 3.69 x 10 in -4 at 1.2 Ro to 3.48 x 10 in -5 at 2.0 Ro.

Table 3 and Figure 9 represent similar computations made for diameter of the entrance aperture of 20 cm, effective wavelength of 530.3 nm, phase grating constant of 5, 10, 20, 50, 100 microns, and micro-roughness of 50 A.
The behaviour of PSF strongly depends on spatial parameters.

Таблица 6

R/Ro	100 мкм		50 мкм		20 мкм		10 мкм		5 мкм	
	(B/Bo) (-3)	lg()	(B/Bo) (-3)	lg()	(B/Bo) (-3)	lg()	(B/Bo) (-3)	lg()	(B/Bo) (-3)	lg()
1.164	0.372	$\bar{4}.570$	0.370	$\bar{4}.568$	0.369	$\bar{4}.566$	0.368	$\bar{4}.566$	0.368	$\bar{4}.566$
1.328	0.163	4.212	0.161	4.208	0.160	4.204	0.159	4.202	0.159	4.202
1.492	0.098	5.991	0.096	5.980	0.094	5.972	0.093	5.970	0.093	5.969
1.656	0.067	5.828	0.065	5.810	0.063	5.800	0.063	5.796	0.062	5.794
1.820	0.050	5.699	0.047	5.676	0.046	5.660	0.045	5.654	0.045	5.652
1.984	0.039	5.592	0.036	5.560	0.035	5.540	0.034	5.536	0.034	5.530

Таблица 7

R/Ro	100 мкм		50 мкм		20 мкм		10 мкм		5 мкм	
	(B/Bo) (-3)	lg()	(B/Bo) (-3)	lg()	(B/Bo) (-3)	lg()	(B/Bo) (-3)	lg()	(B/Bo) (-3)	lg()
1.164	0.389	$\bar{4}.590$	0.378	$\bar{4}.578$	0.372	$\bar{4}.570$	0.370	$\bar{4}.568$	0.369	$\bar{4}.566$
1.328	0.180	4.256	0.169	4.228	0.163	4.212	0.161	4.208	0.160	4.204
1.492	0.116	4.065	0.104	4.018	0.097	5.988	0.095	5.979	0.094	5.973
1.656	0.085	5.931	0.074	5.868	0.067	5.824	0.064	5.809	0.063	5.800
1.820	0.068	5.835	0.057	5.752	0.049	5.693	0.047	5.672	0.046	5.662
1.984	0.058	5.764	0.046	5.662	0.039	5.585	0.036	5.558	0.035	5.542

Таблица 8

R/Ro	100 мкм		50 мкм		20 мкм		10 мкм		5 мкм	
	(B/Bo) (-3)	lg()	(B/Bo) (-3)	lg()	(B/Bo) (-3)	lg()	(B/Bo) (-3)	lg()	(B/Bo) (-3)	lg()
1.164	0.487	$\bar{4}.688$	0.427	$\bar{4}.630$	0.391	$\bar{4}.592$	0.380	$\bar{4}.580$	0.374	$\bar{4}.573$
1.328	0.282	4.450	0.220	4.342	0.183	4.262	0.171	4.233	0.165	4.218
1.492	0.221	4.344	0.157	4.196	0.118	4.072	0.106	4.026	0.099	5.998
1.656	0.193	4.286	0.128	4.107	0.088	5.946	0.075	5.875	0.069	5.836
1.820	0.179	4.253	0.112	4.049	0.072	5.854	0.058	5.763	0.051	5.710
1.984	0.171	4.233	0.102	4.008	0.061	5.786	0.047	5.676	0.041	5.608

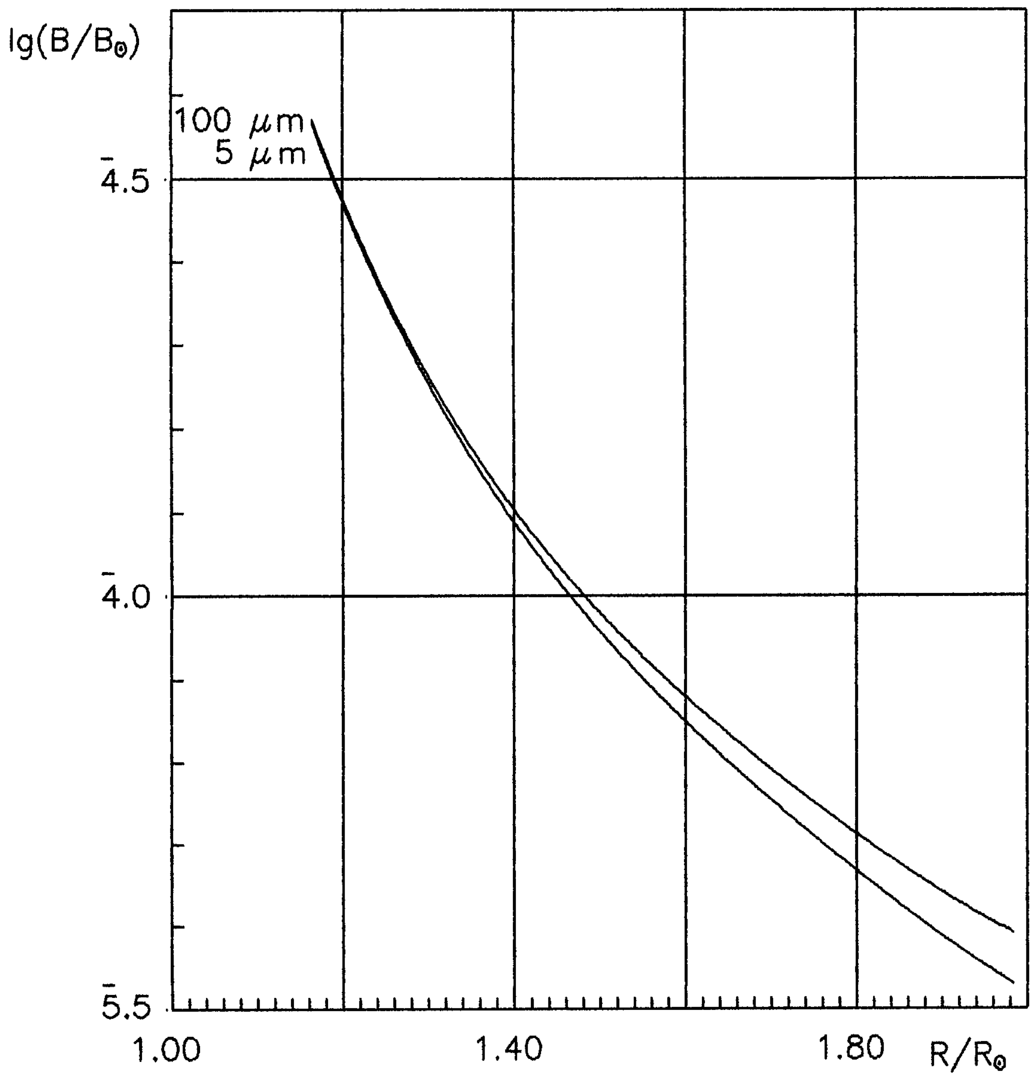

Figure 7. Azimutally averages PSF of the coronagraphic device computed for the diameter of the entrance aperture of 20 cm, effective wavelength of 530.3 nm, micro-roughness of 10 A, and phase grating constant of 5, 10, 20, 50, 100 micron. It's seen that PSF does not practically depend on spatial structure of micro-roughness.

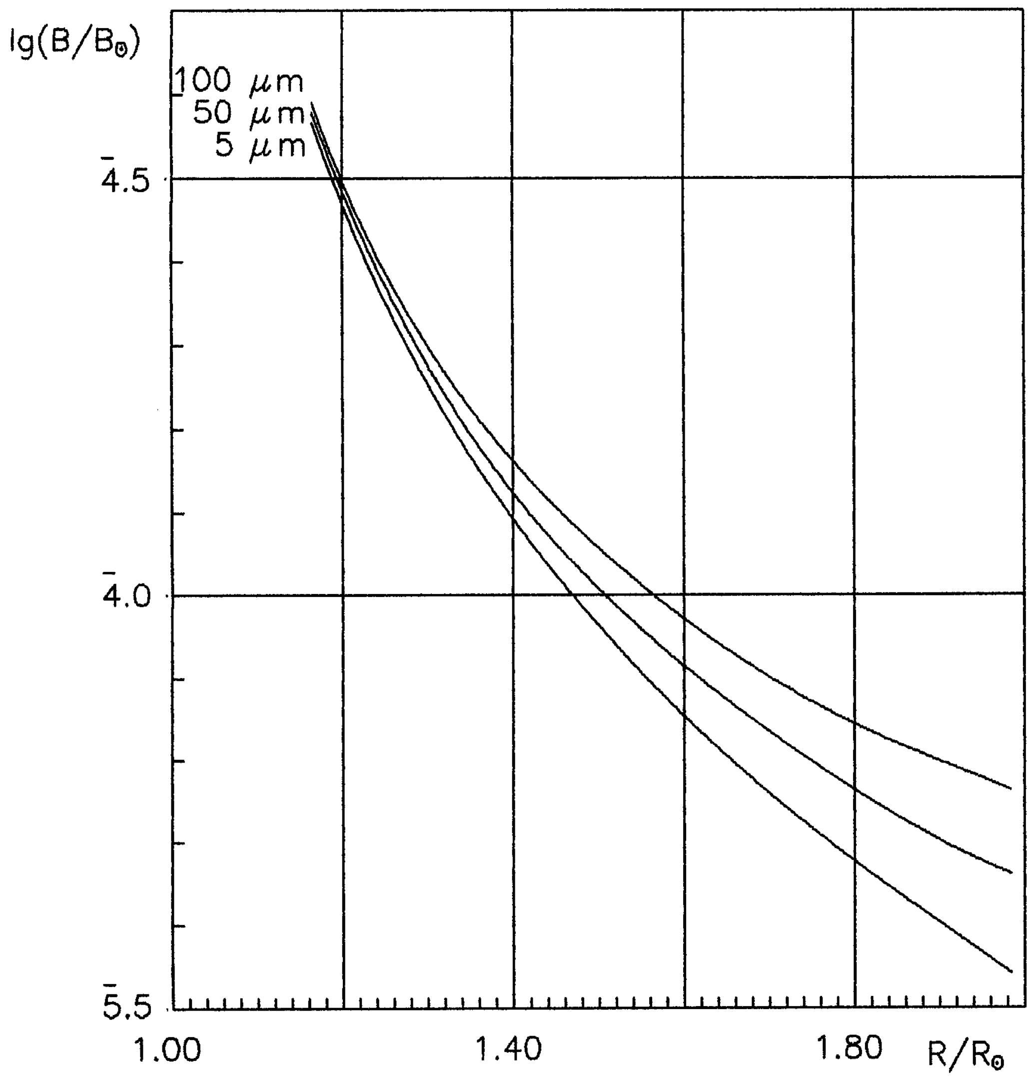

Figure 8. Azimutally averages PSF of the coronagraphic device computed for the diameter of the entrance aperture of 20 cm, effective wavelength of 530.3 nm, micro-roughness of 20 A, and phase grating constant of 5, 10, 20, 50, 100 micron. It's seen that PSF depends on spatial structure of micro-roughness.

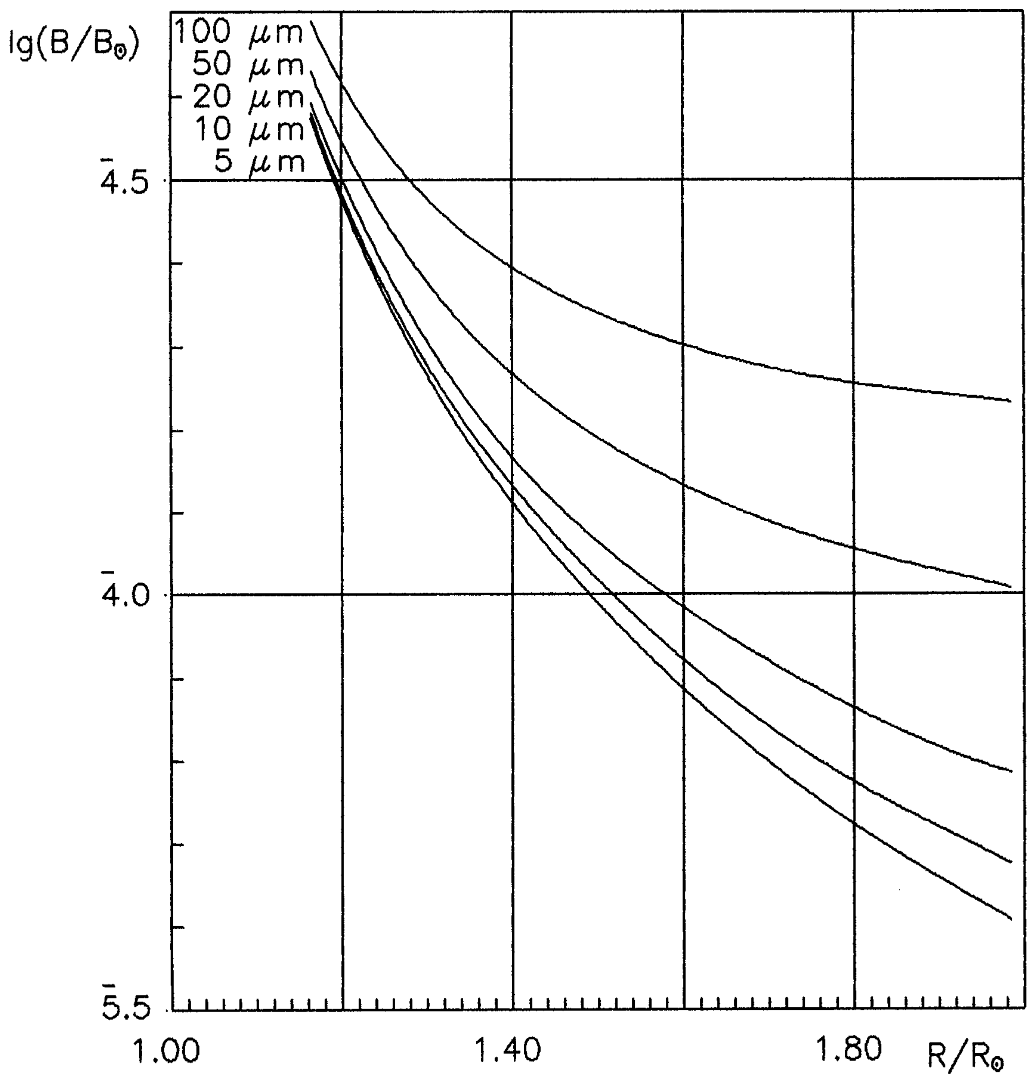

Figure 9. Azimutally averages PSF of the coronagraphic device computed for the diameter of the entrance aperture of 20 cm, effective wavelength of 530.3 nm, micro-roughness of 50 A, and phase grating constant of 5, 10, 20, 50, 100 micron. It's seen that PSF does not practically depend on spatial structure of micro-roughness.

5. Summary

The level of scattered light caused by regular micro-relief with micro-roughness less than or equal to 10 A does not practically depend on spatial parameters in the range of 1.2-2.0 Ro.
The level of scattered light caused by regular micro-relief with roughness greater than or equal to 50 A strongly depends on spatial parameters.

Comparative analysis of measurements of micro-relief of the primary optics of the device shown in Section 3 with the numerical modeling presented in Section 4 results in conclusion that the expected level of the stray light of the device in the range of 1.2-2.0 Ro would not exceed 10 in -4. On the average at 1.6 the stray light would be less than 7 x 10 in -5 allowing direct detecting the faint objects near bright ones while magnitude difference of 12 being.

6. References

Beckmann P., Spizzichino A. (1963), "The scattering of Electromagnetic Waves from Rough Surfaces", Oxford: Pergamon Press, p. 492.

Faure-Geors H., Maystre D., and Roger A. (1988), Journal of Optics (Paris), vol. 19, N 2, p. 51.

Nagaoka H. 1920, vol 51, N 2, p. 73

Toporets A.S.(1988), "Optika sherokhovatykh poverkhnostei" ("Optics of Rough Surfaces"), Leningrad, Mashinostroenie, p. 191.

Romanov A.D., Starichenkova V.D., Fes'kov A.I., Folomkin I.P. (1991), Optiko-mechanicheskaya promyshlennost', N 6, p. 11.

Wazerell W. (1983), "Estimation of Image quality" in "Development of Optical Systems" in Shennon R. and Wint G. (eds), Russian translation, MIR, p. 430.